

**A NEW REAL – TIME FAULT DETECTION
METHODOLOGY FOR SYSTEMS UNDER TEST**

PHASE I REPORT

SUBMITTED BY:

**DR. ROGER W. JOHNSON, Ph.D., PE
ASSOCIATE PROFESSOR
MECHANICAL, MATERIALS AND
AEROSPACE ENGINEERING
UNIVERSITY OF CENTRAL FLORIDA
ORLANDO, FL 32816**

SEPTEMBER 19th, 1998

CONTRIBUTING GRADUATE STUDENTS:

**SANJAY JAYARAM
RICHARD A. HULL**

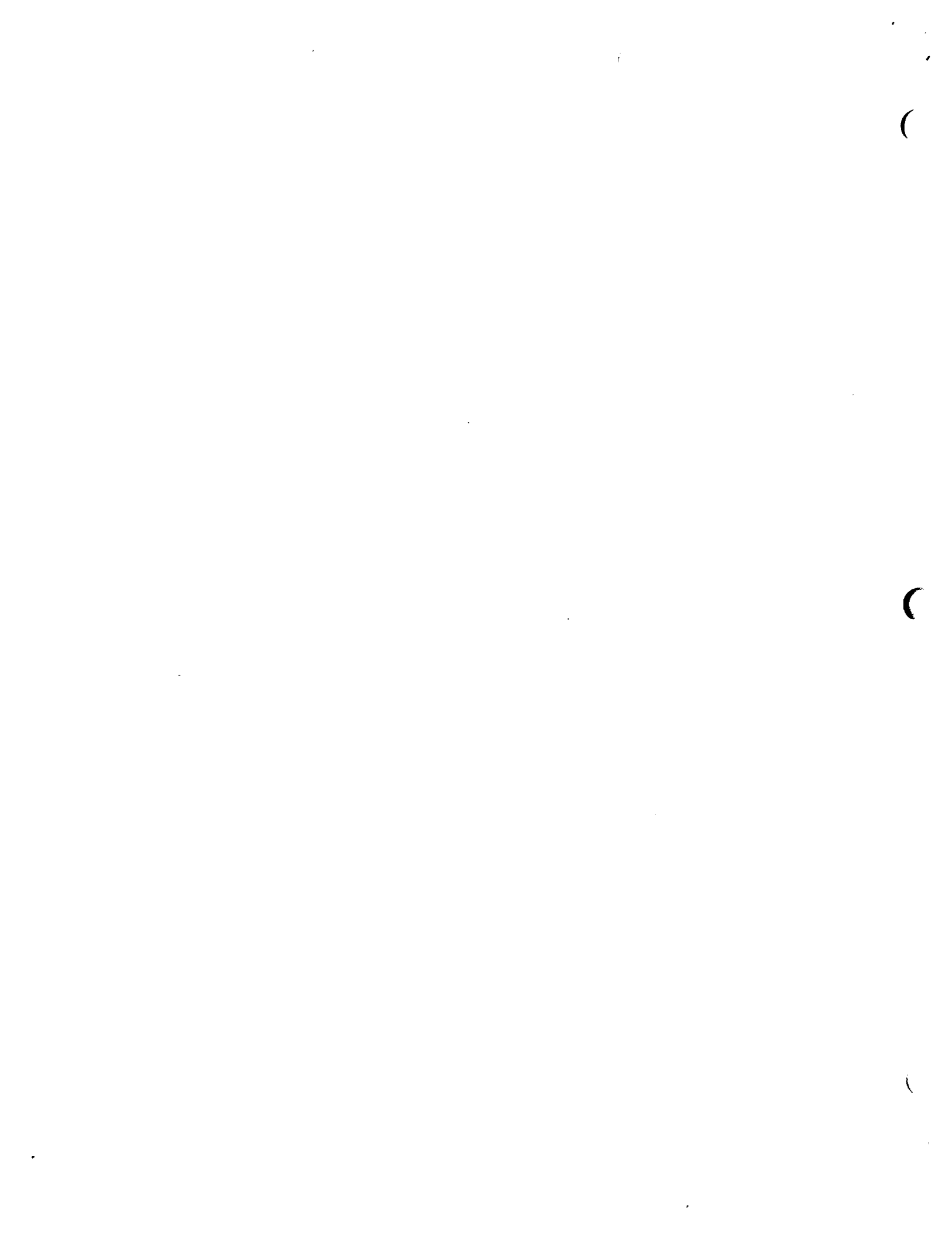


TABLE OF CONTENTS

1. SUMMARY.....	1
2. FLIGHT CONTROL.....	2
2.1 Introduction.....	2
2.2 Statement of Work.....	2
2.3 Objectives	3
2.4 Approach	4
2.5 Flight Control Example	4
2.6 System Identification Using MATLAB.....	7
2.7 Error Detection Filter.....	13
2.8 Detection Filter Algorithm	14
3. KALMAN FILTERING FOR SIGNAL CONDITIONING	17
3.1 Kalman Filter Formulations.....	18
3.2 Study on Optimal Trajectories of Model State Variables.....	21
3.3 Calculation of Optimal Equations	21
4. SIMULATION RESULTS	26

5. LIST OF REFERENCES 30

APPENDIX A

Input – Output Data of Pitch Actuator Controller Test Sequence Used (Figure)

1.0 SUMMARY

The subject emphasized herein is application of A New Real – Time Fault Detection Methodology for Systems Under Test (SUT) applied to data from the actuator of pitch gimbal of a launch vehicle. The technology innovations planned here are software intensive and perfectly compatible with the open physical architecture of existing monitoring devices and the automated control system of Systems Under Test (SUT). Each technology enhancement deals with adding a technical capability without modifying existing physical capabilities (unless desired). The essential objective of this research is to provide these technical enhancements by handling and evaluating test data in a different manner. This equates to operational modifications such as using recursive algorithms rather than data smoothing; the use of computer data comparison and evaluation techniques instead of monitoring and using human operators for controlling mundane test data sequences. To summarize results based on simulations, the error detection filter developed is viewed as a viable tool for monitoring and test and evaluation environment. The algorithm also includes the capability to monitor and detect errors during the steady state response of the system. Some simulation results also shows the ability to use this error detection filter algorithm to develop a database of transient response modes which could then be used as a comparison with actual system responses in real time.



2 – FLIGHT CONTROL

2.1 - INTRODUCTION

The complex automatic systems so widely employed in modern industry can consist of hundreds of inter-dependent working parts, which are individually subject to malfunction or failure. It is therefore necessary to provide the required operation of the entire system by a *scheme of monitoring* which detects a fault as it occurs, thereby identifying the malfunction of the faulty component. The principal concern here is this monitoring function, i.e., the detection, prediction and identification of faults during on-line (real-time) operation of a dynamic system.

2.2 STATEMENT OF WORK

Upon studying and analyzing the previous work done by various engineers on fault detection systems, emphasis is given here on a simpler and more effective means of automatic fault detection methodology which applies the basic principles of identifying the system and using the model based simulations for detecting failures in the system components. In the next section, the approach taken is discussed.

The purpose of this research is focussed on the identification/demonstration of critical technology innovations that will be applied to various applications viz. Detection of automated machine Health Monitoring (HM), real-time data analysis and control of Systems Under Test (SUT). This new innovation using a *High Fidelity Dynamic Model-based Simulation* (HFDMS) approach will be used to implement a real-time monitoring, Test and Evaluation (T&E) methodology including the transient behavior of the system under test. The unique element of this process control technique is the use of high fidelity, computer generated dynamic models to replicate the behavior of actual Systems Under Test (SUT). It will provide a dynamic simulation capability that becomes the reference truth model, from which comparisons are made with the actual raw/conditioned data from the test elements.

The insertion of this new concept for Health Monitoring (HM) into existing automated monitoring and control systems will provide a real-time, intelligent command and control system which has the capability to monitor and observe transient behavior along with the *dynamic parameters* of the systems being operated. Current test capability cannot measure the dynamic behavior of SUT in real time. Abnormal dynamic properties are indicators of an out of tolerance performance of the SUT; they can be a predictor of impending failures in those systems. This feature adds a new dimension to existing test control mechanizations that will greatly enhance the visibility of the "system state" which, in turn, increases the reliability of test and evaluation process over those currently in use. This processing technique also promises the real time detection of abnormal data flow conditions and the automatic identification of the specific "state" causing the fault condition. This attribute will speed up diagnostic analysis to seconds rather than minutes/hours, thus reducing significantly, fault detection and diagnosis.

2.3 OBJECTIVES

Activities attendant to "industry needs" in the area of intelligent launch command and control automated vehicle check-out and system monitoring will be articulated to the growing class of commercial launch vehicles. The characterization for the next step in evolving the existing launch control processes to a more automated posture is to embed these new technical innovations, which makes a *high fidelity, dynamic model based simulation* methodology possible into an automated control system. This effort will remove the operator from all mundane process control procedures, and let the computer actively control and sequence the subsystem or system under test. It will also provide automatic detection of out of tolerance signal flow and furnish the launch operator a notion of how close a measurement is out of tolerance in near real time. Taking into consideration the state-of-technology, the current status of existing and emerging vehicle launch control processes, and the requirements necessary to design an automated, real-time methodology compatible to these systems, a set of objectives are identified to satisfy these projected needs with selected technology innovations.

The following objectives will describe the scope of this research:

1. Identifying the System that is under test and developing a High Fidelity Dynamic Model using the input output data sequence of the actual system.
2. Formulate and apply a new innovation using a High Fidelity Dynamic Model based Simulation approach to implement a real time monitoring system for automating a detection system for detecting an “abnormal signal flow” in the Engine Flight Control System (in particular, the actuator of the pitch axis).
3. Use a Kalman Filter estimation mechanization to reduce raw measurement error before correlation between simulated and actual responses are generated.

2.4 APPROACH

The approach taken in the development of detection methodology for automating the control system is to employ High Fidelity Dynamic Model Based Simulation (HFDMS) method to conduct Test and Evaluation (T&E) procedures. This new innovation of using Dynamic models (i.e. those that include the characteristic differential equations along with their dynamic parameters) to replicate the behavior of the actual system under test, results in a dynamic simulation capability that becomes the reference or truth model, from which, comparisons are made with the actual raw data from test elements. If detection of an “abnormal flow” is triggered, an automatic hand-over to the designated diagnostic component model is implemented for resolution [Ref: 3 and 4].

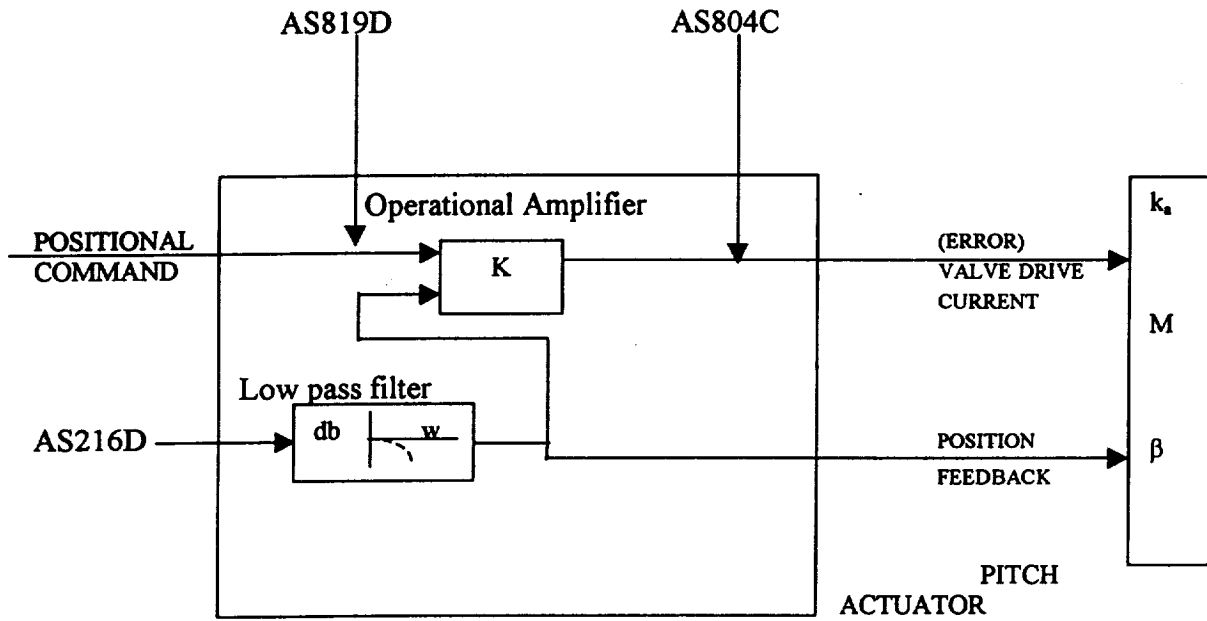
2.5 FLIGHT CONTROL EXAMPLE

A real – time monitoring and error detection algorithm is developed for application with a missile control system actuator. A second order discretized model of a first stage rocket engine pitch gimbal actuator system is developed. An error detection algorithm and filtering approach is then developed which compares the model output to in-coming data in real-time. A recursive approximation to the mean square error (MSE) is obtained via a discrete low pass filter and used with a dynamic threshold detection algorithm. A novel feature of this method is the use of model rate information and a matched filter approach to generate the dynamic error threshold. This enables good detection results to be

obtained for errors in both transient and steady state response characteristics. Actual pre-launch data is then used to verify the performance of this error detection filter [Ref: 3].

ACTUATOR SUBSYSTEM MODEL:

The engine pitch controller will be analyzed. The description and block diagram (Laplace transform) for this control loop is shown in Fig (1) and (2) respectively.



AS819D: Test sequence input.

AS804C: Servo error signal.

AS216D: Actuator response.

Figure (1): Description of engine pitch actuator system.

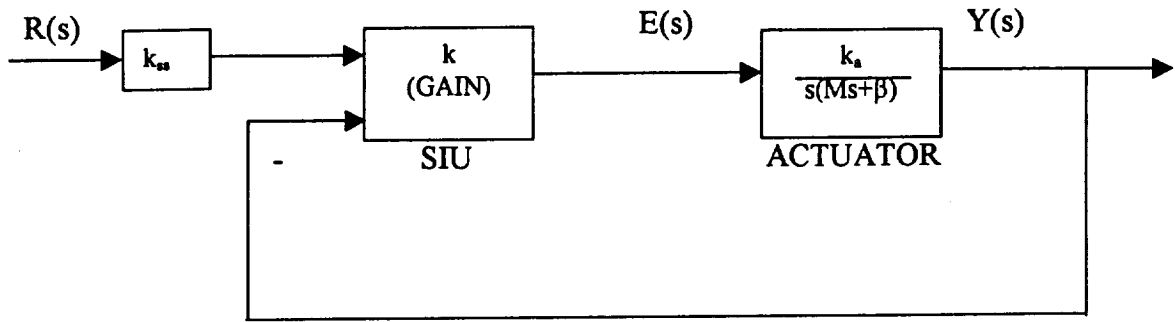


Figure (2): Block diagram of engine pitch actuator system

The linear closed loop transfer function $Y(s)/R(s)$ for the system in Fig (2) is [Ref. 1, 2 and 9]:

$$\frac{Y(s)}{R(s)} = \frac{k_{ss}\omega_n^2}{s^2 + 2\zeta\omega_n s + \omega_n^2}$$

where :

$$\omega_n = \sqrt{\frac{k_a k}{M}}$$

$$\zeta = \frac{\beta}{2\sqrt{Mk_a k}}$$

Parameters:

$Y(s)$ = Laplace transform of the output signal.

$R(s)$ = Laplace transform of the input signal.

ζ = Damping factor.

ω_n = Natural frequency (rad/sec)

k_{ss} = Steady state gain

M = Mass of actuator/gimbal

β = Damping coefficient of actuator

k_a = Actuator gain

k = Servo Inverter Unit gain

The engine pitch gimbal actuator system can therefore be modeled as a second order system. This model was obtained by using the “*System Identification*” Toolbox for MATLAB. The description of the identification methodology is discussed in next section. The actual raw data is obtained from a preflight pitch gimbal test sequence shown in APPENDIX A. This figure shows the test sequence input commands (AS 819D), the actuator response (AS 216D), and the servo error signal (AS 804C). The input command sequence consists of a step command, followed by a ramp command that overdrives the actuator into its hard limit, then a return to zero command. This sequence is repeated in the negative direction. These rates corresponds to sample times of 0.007875 seconds.

2.6 SYSTEM IDENTIFICATION USING MATLAB

As stated in the previous section, System Identification toolbox was used to model the system under test. The basic steps in system identification:

- a. Collection of raw input-output data sequence from the actual system to be identified.
- b. Selecting and defining a model structure within which a model is to be estimated.
- c. Computation of best model with a given criterion of fit for the known input-output data.
- d. Examination of the properties of model thus selected/estimated.

The control system identification deals primarily with four different types of Model structures:

- a. ARX Model structure
- b. ARMAX Model structure
- c. Instrumental variable model structure
- d. Box-Jenkins Model structure.

In this research, we used the ARX model structure since it was simple and better for second order system identifications. Hence a brief discussion is made regarding estimating the parameters of an ARX model.

The parameters of an ARX structure in a general sense are given by:

$$A(q)y(t) = B(q)u(t - nk) + e(t)$$

Here $A(q)$ is an $ny \times ny$ matrix whose entries are polynomials in the delay operator q^{-1} . It can be represented as:

$$A(q) = I_{ny} + A_1q^{-1} + \dots + A_{na}q^{-na}$$

Similarly $B(q)$ is an $ny \times nu$ matrix

$$B(q) = B_0 + B_1q^{-1} + \dots + B_{nb}q^{-nb}$$

assumption is made that we already know the array z that consists of input/output data from the system

$$z = [y \ u]$$

For estimating the parameters $A(q)$ and $B(q)$ of the ARX model, use the function *arx*:

The command is given by:

$$th = arx(z, [na \ nb \ nk])$$

Here na , nb and nk are the corresponding orders and delays that define the exact model structure. The function *arx* implements the least squares estimation method using the MATLAB for overdetermined linear equations. The input variables y and u are column vectors that contain output and input data. The resulting estimated model is contained in "*th*" which is called the "*theta format*". This is the basic format for representing models in the System Identification Toolbox. It collects information about the model structure and the orders, delays, parameters and estimated co-variances of the parameters into a matrix. The theta format can further be translated into any other useful model representations like Transfer Function representation or State Space representation. For more details in this subject, reference can be made to [25 and 14].

The model representation obtained by using System Identification Toolbox is obtained as:

Transfer function representation:

$$\frac{C(s)}{R(s)} = \frac{0.8125s + 0.4145}{s^2 + 17.66s + 1.554}$$

State space representation:

$$A = \begin{bmatrix} -17.66 & 1 \\ -1.554 & 0 \end{bmatrix} \quad B = \begin{bmatrix} 0.8125 \\ 0.4145 \end{bmatrix} \quad C = [1 \ 0] \quad D = 0$$

Discrete transfer function representation:

$$\frac{Y(z)}{R(z)} = \frac{0.0037326z + 0.0035932}{z^2 - 1.8921z + 0.89209}$$

Figure (3) shows a simple simulation block diagram of the Pitch actuator model with file inputs [Ref: 11 and 13].

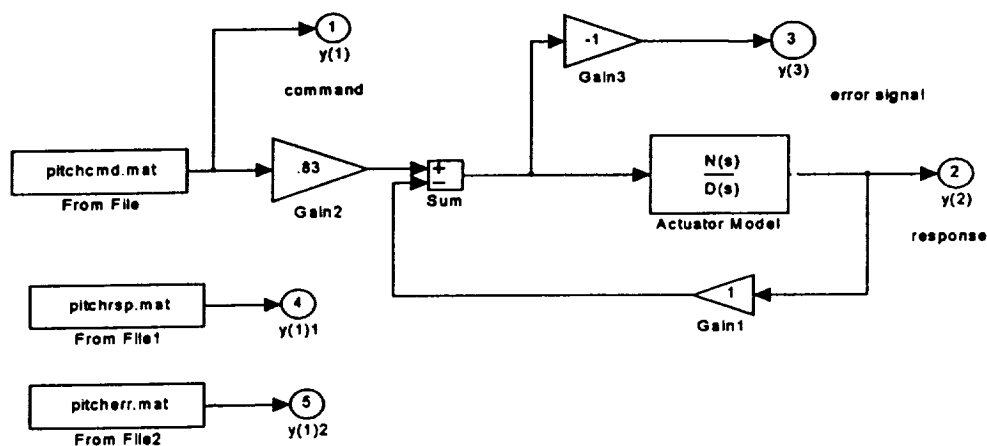


Figure (3) : Pitch controller simulation model with input files.

The parameters found for the nominal system are:

$$\begin{aligned}\zeta &= 0.776 \\ \omega_n &= 11.378 \text{ rad/sec} \\ k_{ss} &= 0.83\end{aligned}$$

The Figure (4) represents the data provided, which shows the characteristic response of slightly under-damped second order system. This magnified figure also shows that there is a digital noise present in the command and response data.

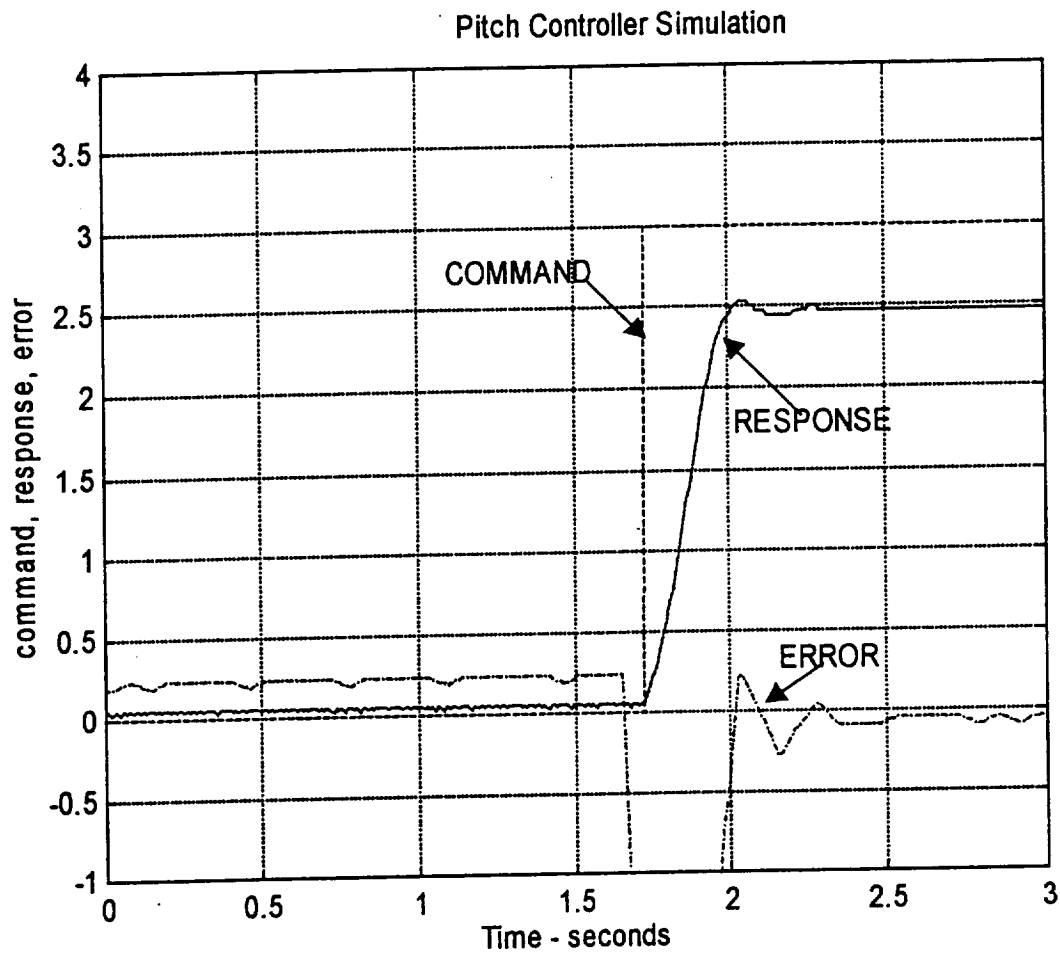


Figure (4): Pitch actuator controller.

Figure (5) shows the block diagram of the resulting discretized pitch actuator model. The inner block shows the discrete version of the unity gain open loop transfer function, taken as the direct Z transform, using sampling time $T = 0.007875$ seconds of the transfer function:

$$\frac{Y(s)}{R(s)} = \frac{\omega_n^2}{s^2 + 2\zeta\omega_n s}$$

which yields:

$$\frac{Y(z)}{R(z)} = \frac{0.0037326}{z^2 - 1.8921z + 0.89209}$$

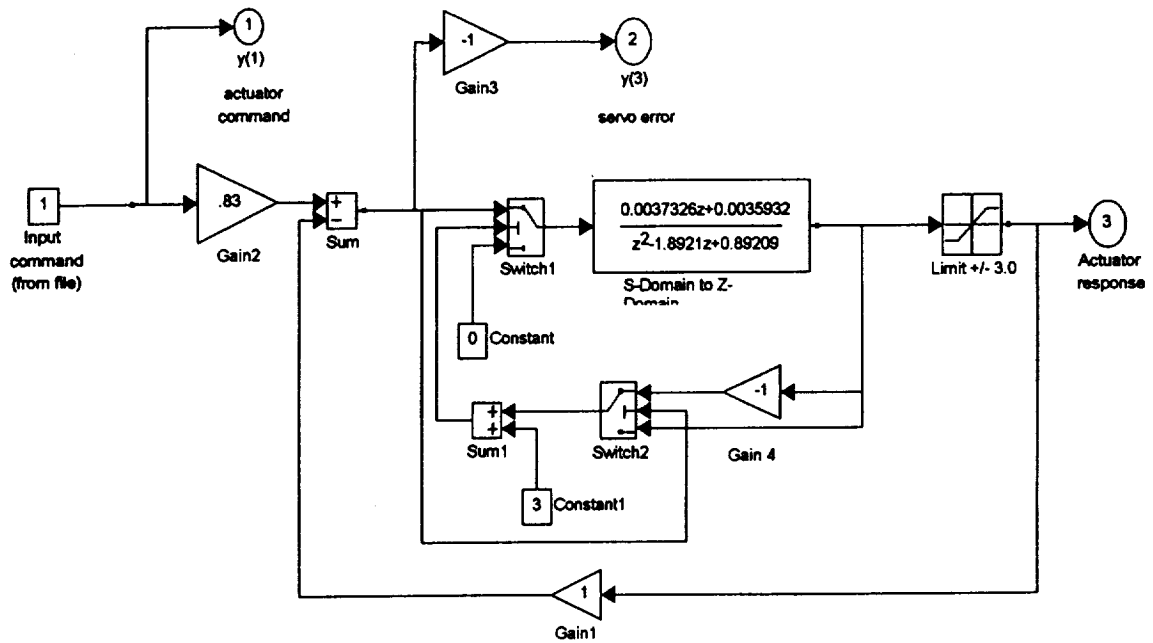


Figure (5): Pitch actuator controller model – discrete transfer function (input and output limited saturation protection).

The output of this transfer function is then limited to a ± 3.0 degrees of travel before feeding it back to close the loop. The switches shown in the Figure are used to set the input to the transfer to zero, whenever the output of the transfer function is being driven into the limit. The steady state gain appears as gain1 in the diagram and is applied to the input command signal. Outputs are provided from the subsystem model to give actuator response, actuator rate, and servo error [Ref: 11 and 13].

The accuracy of this model is illustrated in Figure (6) and (7), which overlay the input command data (from the file), the actual actuator response data (from the file) and the actual model response (from the simulation). We can observe that the model is accurate enough to demonstrate the methodology of the error detection filter algorithm that is discussed in the next section.

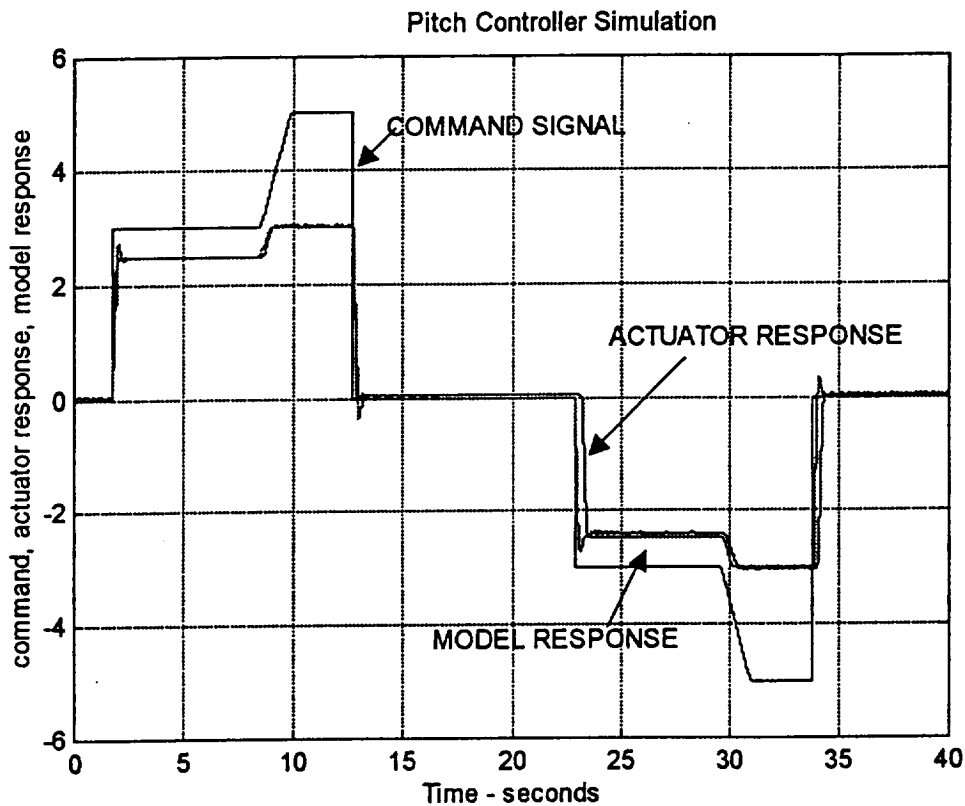


Figure (6): Pitch actuator controller simulation showing model response and actuator response (from file).

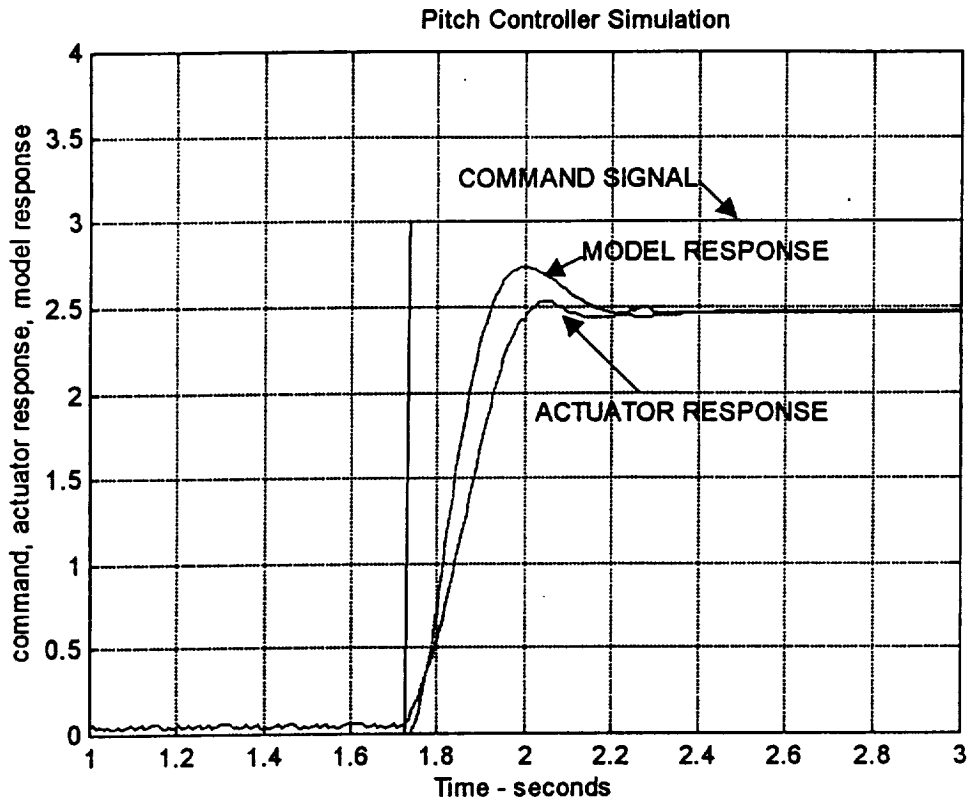


Figure (7): Pitch actuator controller simulation – model response and actuator response expanded view.

2.7 ERROR DETECTION FILTER

The error detection filter algorithm developed in this study works by comparing the actual actuator response data to the response of the actuator subsystem model to the actual actuator command data. From the output of the error detection filter, mean squared error is computed. This is then compared with the variable threshold which is the “model rate of change”. If the mean squared error is less than the threshold value, error detect will be “zero”; if the mean squared error value is more than the threshold value, error detect will be “one”, which triggers the fault detection system and a fault is detected.

2.8 DETECTION FILTER ALGORITHM

A block diagram of the error detection filter process is shown in the Fig (8), which represents the simulation diagram for this research study. As shown in this figure, the actual command data (obtained either from on line or from a computer file) is used to drive the pitch actuator model. The model response and rate of change information are input to the error data detection filter subsystem, along with the actual response data (obtained either on line, or from a computer file). For future simulation purposes, a band limited white noise function is shown in summation with the response data. Other blocks in this diagram simply represent output ports, which makes the data available for plotting and recording. (Figure shown in next page).

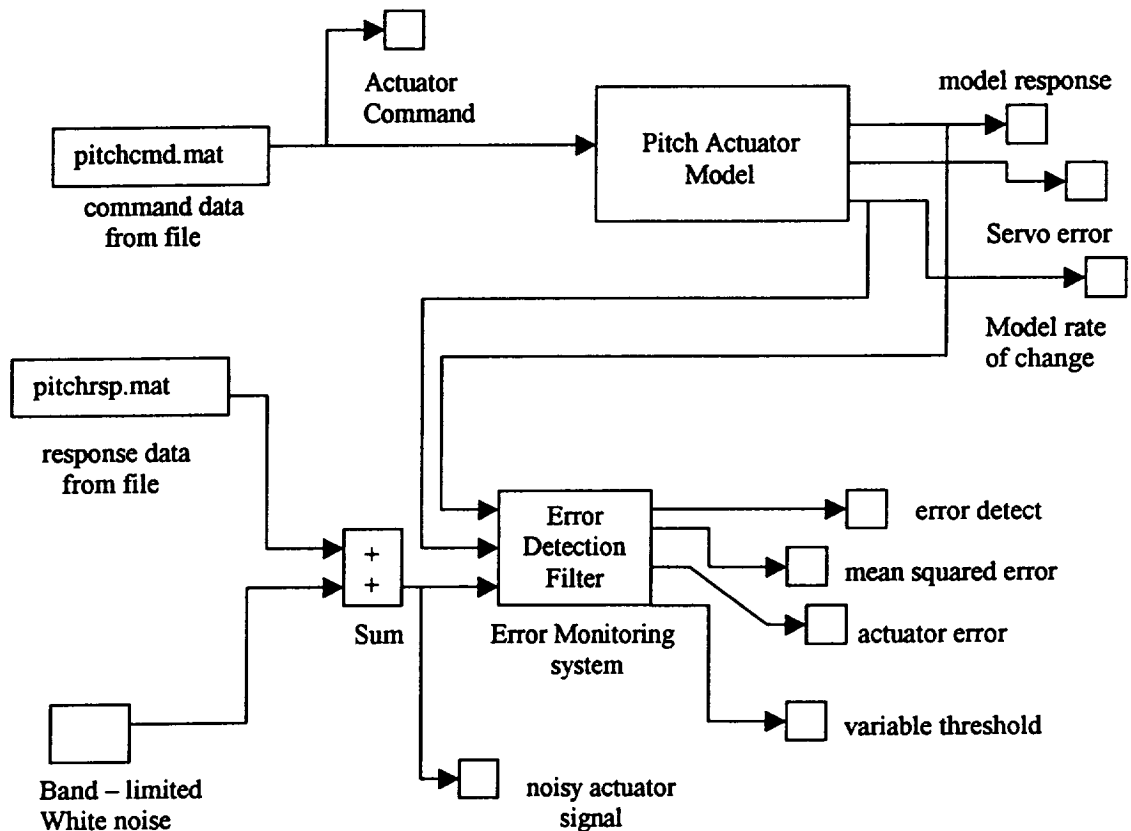


Figure (8): Pitch controller simulation – file inputs – discrete transfer function model

A detailed block diagram of only the error detection filter is shown in Fig (9). The error between the system response data and the model response is squared and passed through a discrete low pass filter. This provides an approximation to the expected (or average) value of the mean squared error (MSE). This mean squared error value is then compared to a threshold value and the error detection filter subsystem outputs a “zero” (meaning no error) if the MSE is below the threshold, and a “one” (meaning an error is detected) if the MSE is above the threshold [Ref: 11 and 13].

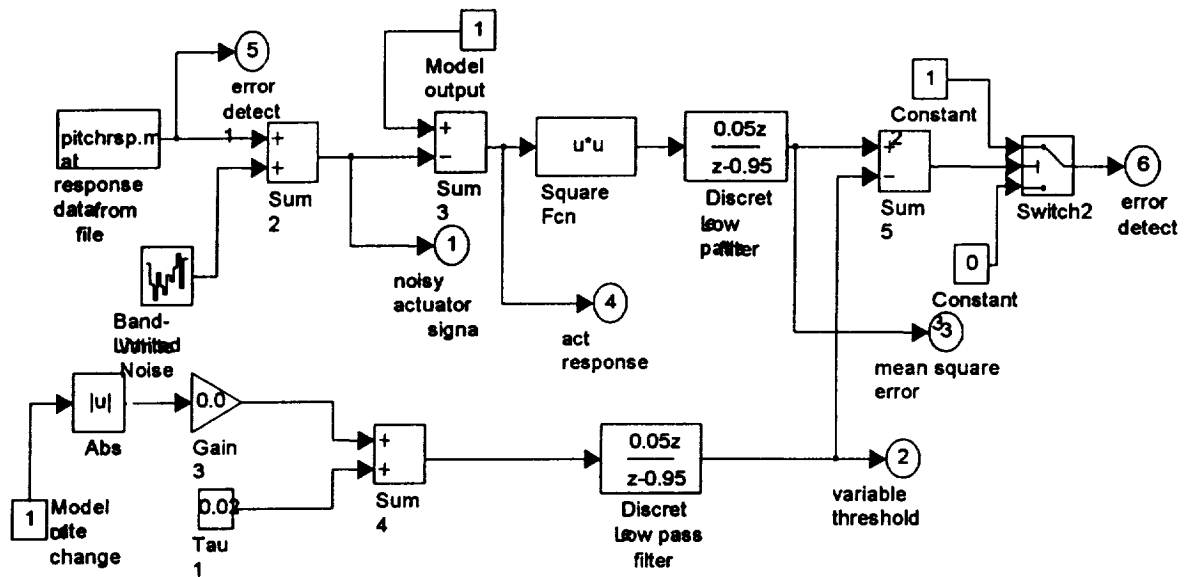


Figure (9): Error Detection Filter – Recursive mean square – Discrete approximation with threshold detection.

A novel feature of this detection algorithm is the use of the model rate information to dynamically adjust the error detection threshold. When the system is in steady state, it is relatively easy to develop a model that accurately represents the system. However, when the system is changing state rapidly, it is more difficult to accurately represent the system, and more error should be tolerated to prevent false detects. Therefore, as shown in the above Figure (9), a dynamic threshold is computed as follows:

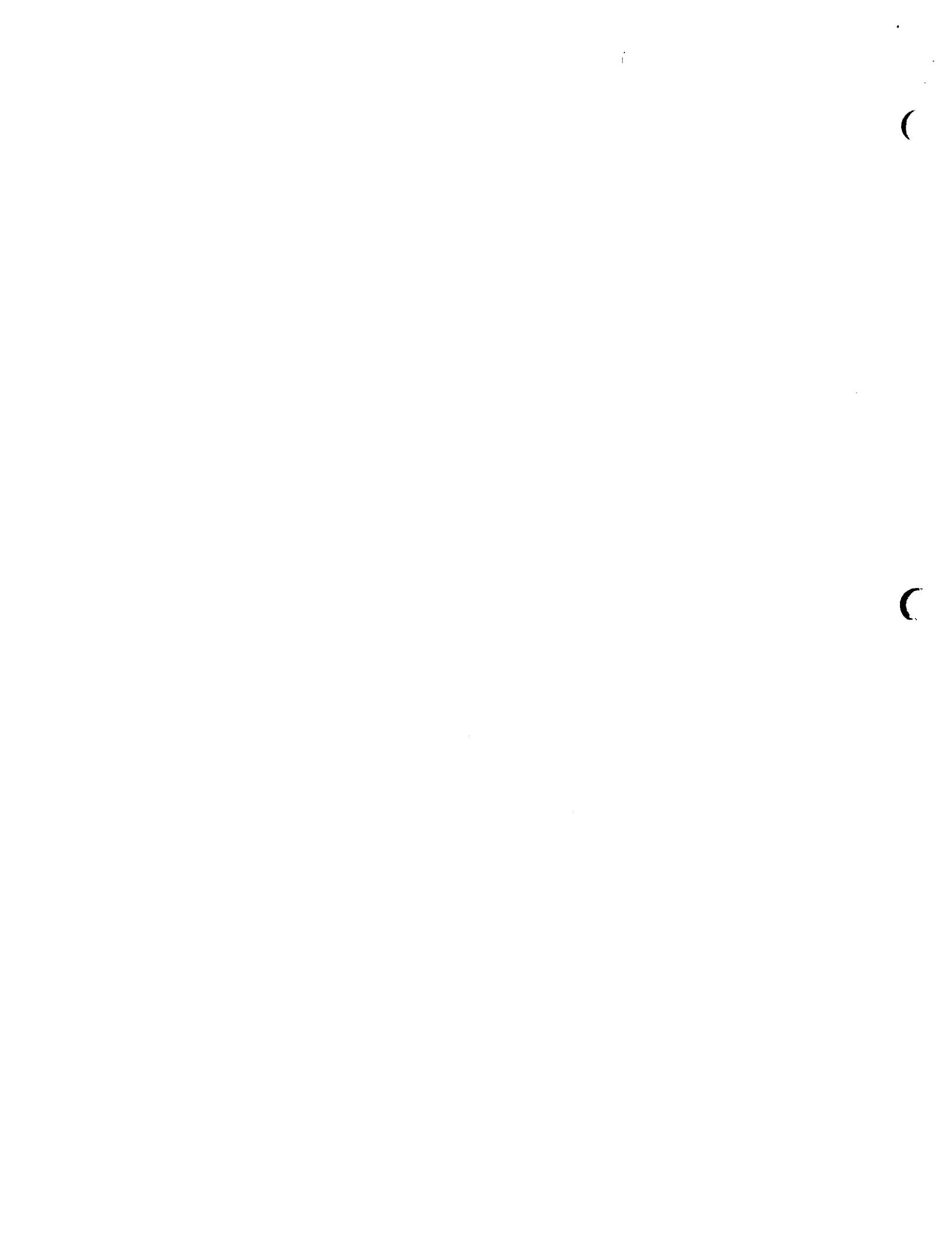
$$\tau = \tau_1 + |y| \tau_2$$

where:

- τ = Dynamic threshold
- y = Model rate of change
- τ_1 = Steady state threshold
- τ_2 = Rate sensitive factor

For this study, the simulation was run for various values of τ_1 and τ_2 and a optimum values for these constants were achieved. It was found that $\tau_1 = 0.02$ and $\tau_2 = 0.04$ worked well.

Finally, it should be noted that the dynamic threshold value itself must be passed through a discrete digital filter matched to the one used to determine MSE, so that the phase lag between the two signals remains matched. This greatly reduces false error detections and allows for tighter setting of the threshold parameters.



3- KALMAN FILTER FOR SIGNAL CONDITIONING

The use of Kalman filter is uniquely structured to condition raw data sequences in real-time. In practice, the following are several cases that can be handled by the recursive procedure:

- i. The state variables can be measured directly; the object will be to filter the noise from the raw measurement before comparison to the nominal model (false detection will be the motivation here).
- ii. The state variables can be measured directly. If several sensors are used to measure the same variable, automatic weighing, based on statistical parameters of the sensors, is applied by the Kalman filter to generate the “best estimate” of that state variable.
- iii. The state variable is impossible to measure directly; this case can be implemented by finding the “best estimate” of those states by using measured data that can be related by a known functional relationship to the desired state variables.

The block diagram of the Kalman filter process is shown in Fig (10).

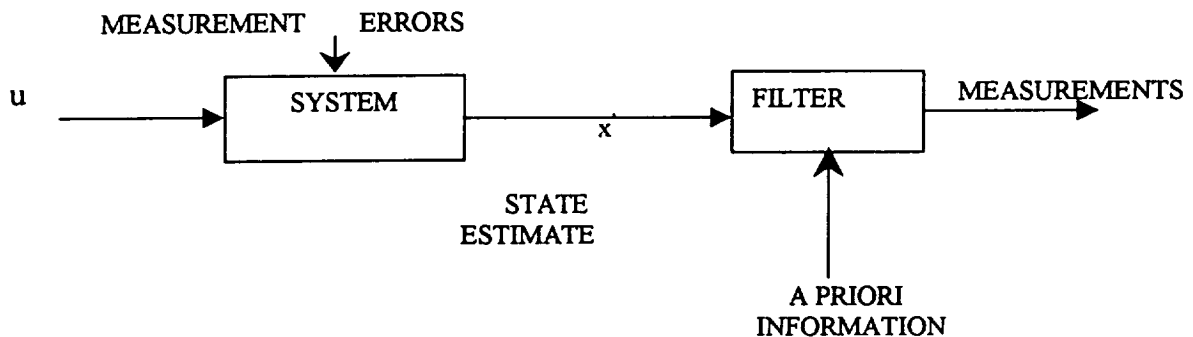


Figure (10): Data flow for filtering process.

3.1 KALMAN FILTER FORMULATIONS [Ref: 5 and 6]

The random process to be estimated is modeled in the form of

$$x_{k+1} = \phi_k x_k + w_k$$

The observation or the output of the system is given by,

$$z_k = H_k x_k + v_k$$

where:

x_k = (nx1) process state vector

ϕ_k = (nxn) state transition matrix

w_k = (nx1) vector, assumed to be white noise with known covariance structure.

z_k = (mx1) vector measurement (output)

H_k = (mxn) measurement to state matrix

v_k = (mx1) measurement error assumed to be white noise with known covariance structure.

The covariance matrices for w_k and v_k vectors are given by Q_k and R_k . Assumption is made that the initial estimate of the process is known at some point of time and this estimate is based on the knowledge of the process. The estimation error is:

And the associated error covariance matrix is:

$$e_k = x_k - \hat{x}_k$$

where \hat{x}_k - priori - estimate

With the known apriori estimate, the updated estimate is found:

$$P_k^- = E[e_k e_k^T] = E[(x_k - \hat{x}_k)(x_k - \hat{x}_k)^T]$$

where:

K_k = The Kalman filter gain

Now the error covariance matrix with the updated estimate is given by:

$$P_k = E[e_k e_k^T] = E[(x_k - \bar{x}_k)(x_k - \bar{x}_k)^T]$$

$$\bar{x}_k = \hat{x}_k + K_k(z_k - H_k \hat{x}_k)$$

In terms of noise covariance, Kalman filter gain (K_k) and H_k , the error covariance is given by:

$$P_k = (I - K_k H_k) P_k^- (I - K_k H_k)^T + K_k R_k K_k^T$$

Now an expression is found for the computation of the Kalman filter gain (K_k) by differentiating the above equation with respect to K since we wish to minimize the trace of P as it is the sum of the mean-square errors of the estimates of all the elements of the state vector. Hence K_k is given by:

$$K_k = P_k^- H_k^T (H_k P_k^- H_k^T + R_k)^{-1}$$

A simple expression can be derived for error covariance matrix from above expressions:

$$P_k = (I - K_k H_k) P_k^-$$

The next step is to make the optimal use of the measurement z_{k+1} . This is accomplished by first updating the process estimate:

$$x_{k+1}^- = \phi_k \bar{x}_k$$

The error covariance matrix associated with updated process estimate is obtained by:

$$e_{k+1}^- = x_{k+1} - x_{k+1}^- = \phi_k e_k + w_k$$

Thus we can write the expression for updated error covariance matrix as:

$$P_{k+1}^- = \phi_k P_k \phi_k^T + Q_k$$

The above equations comprises of Kalman filter recursive equations.

Figure (11) shows the Kalman filter recursive loop structure.

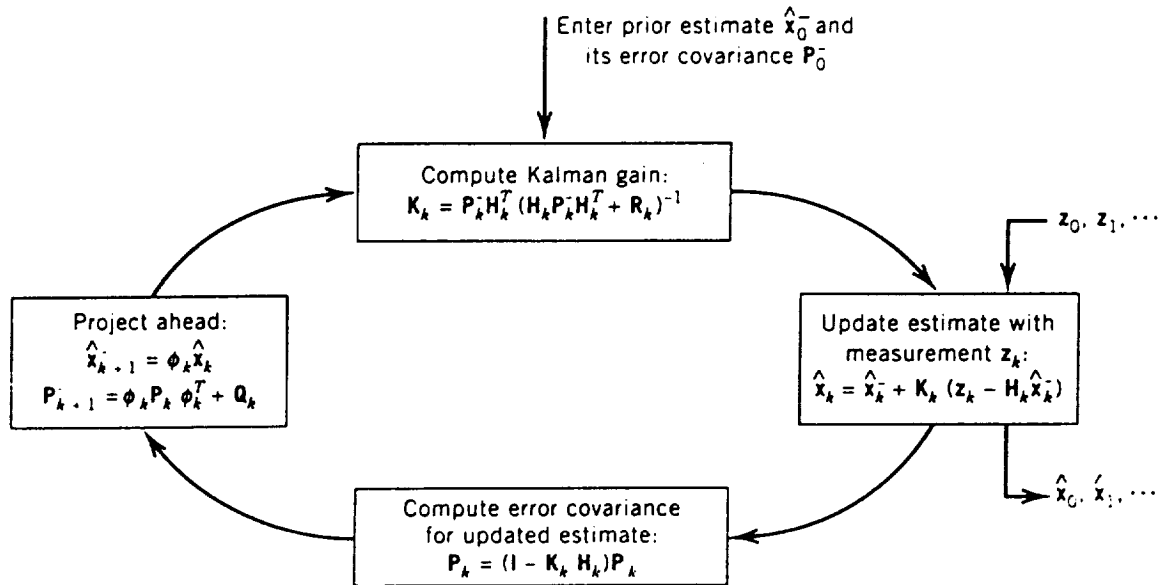


Figure (11): Kalman filter recursive loop.

Now that we are in a stage where the system is identified using the input output data, a model has been developed along with a error detection system and error detection filter algorithms, and a stage has been reached wherein we can study the optimal trajectories of the model state variables, which will help us in validating the developed model in a optimal sense. In other words, we can see from the plots of optimal trajectories with varying initial conditions, that the states and the co-state variables of the model reach steady state values quite quickly and also all the necessary optimal control conditions are satisfied by the state equations. Here study has been made using the state equations and

forming the Hamiltonian equation to see the behavior of the state and co-state trajectories. This is discussed in detail in the next section.

3.2 STUDY ON OPTIMAL TRAJECTORIES OF MODEL STATE VARIABLES

The system modeled has representations in State space and Transfer function forms as:

Transfer Function [Ref: 8]:

$$\frac{C(s)}{R(s)} = \frac{0.8125s + 0.4145}{s^2 + 17.66s + 1.554}$$

State Space:

$$A = \begin{bmatrix} -17.66 & 1 \\ -1.554 & 0 \end{bmatrix} \quad B = \begin{bmatrix} 0.8125 \\ 0.4145 \end{bmatrix} \quad C = [1 \ 0] \quad D = 0$$

3.3 CALCULATION OF OPTIMAL EQUATIONS:

System Equations:

$$\begin{aligned} \dot{x}_1 &= -17.66x_1 + x_2 + 0.8125u \\ \dot{x}_2 &= -1.554x_1 + 0.4145u \end{aligned}$$

Hamiltonian is assumed to be:

$$H(t) = x^T(t)Qx(t) + u^T(t)Ru(t) + p^T(t)Ap(t) + p^T(t)Bu(t)$$

where:

$$Q=I, R=1[\text{assumed}]$$

p = co-state vector

The necessary conditions for optimality are:

$$\begin{aligned} \dot{x}^*(t) &= \frac{\partial H}{\partial p} = Ax^*(t) + Bu^*(t) \\ \dot{p}^*(t) &= -\frac{\partial H}{\partial x} = -Qx^*(t) - A^T p^*(t) \\ \frac{\partial H}{\partial u} &= 0 \end{aligned}$$

Since the system is of order 2x2, the number of optimal equations we get are four, which are:

$$\begin{aligned}\dot{p}_1^* &= -17.66p_1^* + 2x_1^* \\ \dot{p}_2^* &= -1.554p_2^* + 2x_2^* \\ \frac{\partial H}{\partial u} = 0 &= 2u^*(t) + 0.8125p_1^*(t) + 0.4145p_2^*(t) \\ \text{simplifying } \Rightarrow \\ u^*(t) &= -0.40625p_1^*(t) - 0.20725p_2^*(t)\end{aligned}$$

Substituting this optimal control in state equations, we get:

$$\begin{aligned}\dot{x}_1^*(t) &= -17.66x_1^*(t) + x_2^*(t) - 0.33p_1^*(t) - 0.1684p_2^*(t) \\ \dot{x}_2^*(t) &= -1.554x_1^*(t) - 0.1684p_1^*(t) - 0.0859p_2^*(t)\end{aligned}$$

Hence the four optimal differential equations obtained are:

$$\begin{aligned}\dot{x}_1^*(t) &= -17.66x_1^*(t) + x_2^*(t) - 0.33p_1^*(t) - 0.1684p_2^*(t) \\ \dot{x}_2^*(t) &= -1.554x_1^*(t) - 0.1684p_1^*(t) - 0.0859p_2^*(t) \\ \dot{p}_1^* &= -17.66p_1^* + 2x_1^* \\ \dot{p}_2^* &= -1.554p_2^* + 2x_2^*\end{aligned}$$

By solving the above differential equations by the method of finding eigenvalues and eigenvectors, the resulting equations are in the form:

$$\begin{bmatrix} p_1^* \\ p_2^* \\ x_1^* \\ x_2^* \end{bmatrix} = c_1[\bar{x}_1]e^{\lambda_1 t} + c_2[\bar{x}_2]e^{\lambda_2 t} + c_3[\bar{x}_3]e^{\lambda_3 t} + c_4[\bar{x}_4]e^{\lambda_4 t}$$

Where the x 's shown in the above equations are the eigenvectors of the differential equations and λ 's are the corresponding eigenvalues.

A code is written in Matlab to generate various plots for the optimal states, optimal co-states and optimal control trajectories for different initial conditions. The program is shown below, by which for different initial conditions, various values of the constants can be found out:

The matrix of eigenvectors and eigenvalues:

Eigenvectors:

V =

```
-0.3153+ 0.1977i  -0.3153- 0.1977i  -0.0242  -0.0072
-0.0246+ 0.0241i  -0.0246- 0.0241i  -0.5622  0.0513
 0.4474+ 0.8125i   0.4474- 0.8125i  -0.0028  -0.0009
 0.0032- 0.0028i   0.0032+ 0.0028i  -0.8267  0.9987
```

Eigenvalues:

D =

```
-17.6144+ 0.8012i   0   0   0
      0   -17.6144- 0.8012i   0   0
      0   0   -0.1939   0
      0   0   0   -1.4512
```

Matlab Program:

```
%Initial conditions
a=[1 0 0 0];
I=a';
v=[-0.3153+0.1977i -0.3153-0.1977i -0.0242 -0.0072;-0.0246+0.0241i -
0.0246-0.0241i -0.5622 0.0513;0.4474+0.8125i 0.4474-0.8125i -0.0028
-0.0009;0.0032-0.0028i 0.0032+0.0028i -0.8267 0.9987];
V=inv(v);
C=V*I;
C1=C(1,:);
C2=C(2,:);
C3=C(3,:);
C4=C(4,:);
%X1, X2, P1, P2 are the optimal trajectories.
t=[0:0.15:20];
X1=C1*(-0.3153+0.1977i)*exp(-17.6144*t+0.8012i*t)+C2*(-0.3153
-0.1977i)*exp(-17.6144*t-0.8012i*t)+C3*(-0.0242)*exp(
-0.1939*t)+C4*(0.0072)*exp(-1.4512*t);
X2=C1*(-0.0246+0.0241i)*exp(-17.6144*t+0.8012i*t)+C2*(-0.0246
-0.0241i)*exp(-17.6144*t-0.8012i*t)+C3*(-0.5622)*exp(
-0.1939*t)+C4*(0.0513)*exp(-1.4512*t);
P1=C1*(0.4474+0.8125i)*exp(-17.6144*t+0.8012i*t)+C2*(0.4474
-0.8125i)*exp(-17.6144*t-0.8012i*t)+C3*(-0.0028)*exp(-0.1939*t)+C4*(
-0.0009)*exp(-1.4512*t);
```

```

P2=C1*(0.00320.0028i)*exp(17.6144*t+0.8012i*t)+C2*(0.0032+0.0028i)*exp(-
-17.6144*t-0.8012i*t)+C3*(-0.8267)*exp(-0.1939*t)+C4*(0.9987)*exp(-
1.4512*t);
plot(t,X1,'-',t,X2,'.',t,P1,'-.',t,P2,'*')
title('Plot of Optimal Trajectories-State and Costate')
xlabel('time')
ylabel('Optimal Trajectories')
gtext('X1')
gtext('X2')
gtext('P1')
gtext('P2')
gtext('Init Cond: X1=1,X2=1,P1=0,P2=0')

```

Figures (12) and (13) shows plot of optimal trajectories for a set of initial conditions. As described before, the above program can be executed for various combinations of initial conditions.

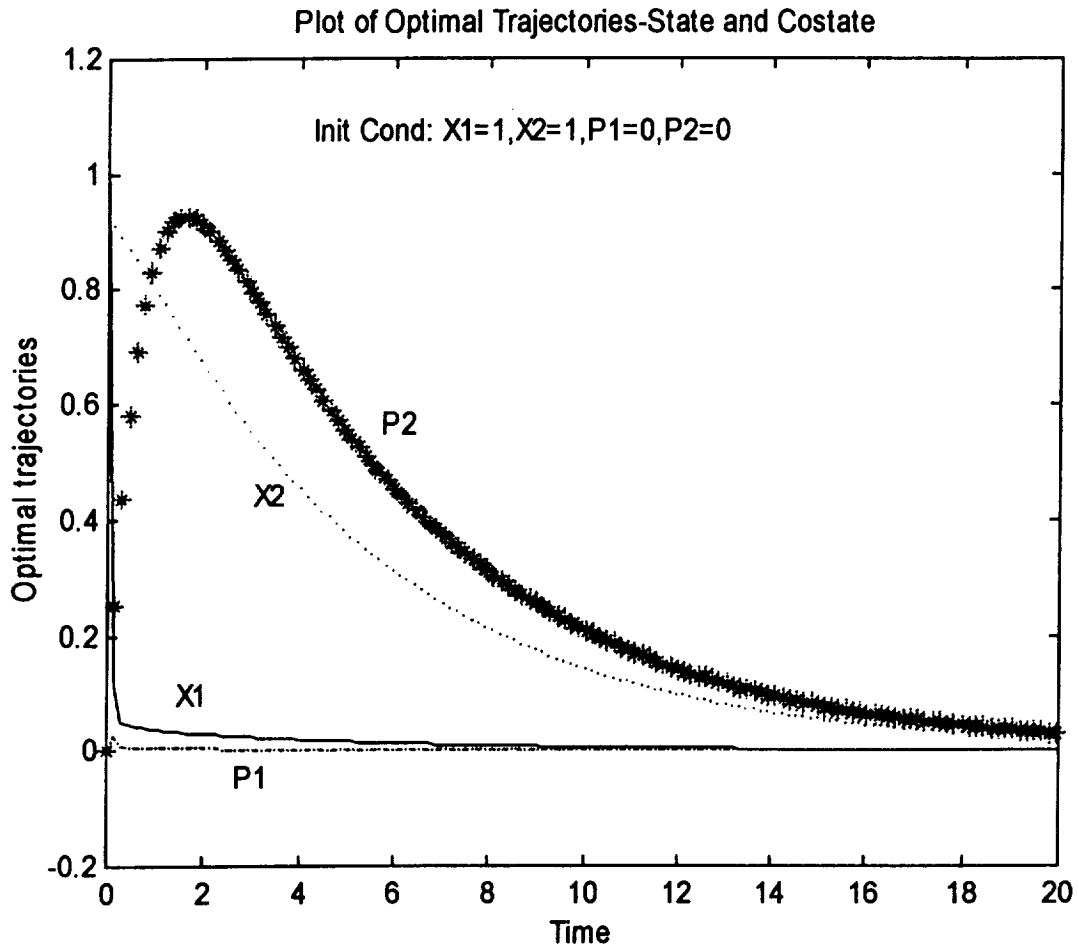


Figure (12): Pitch controller – Optimal trajectories of state and co-state vectors

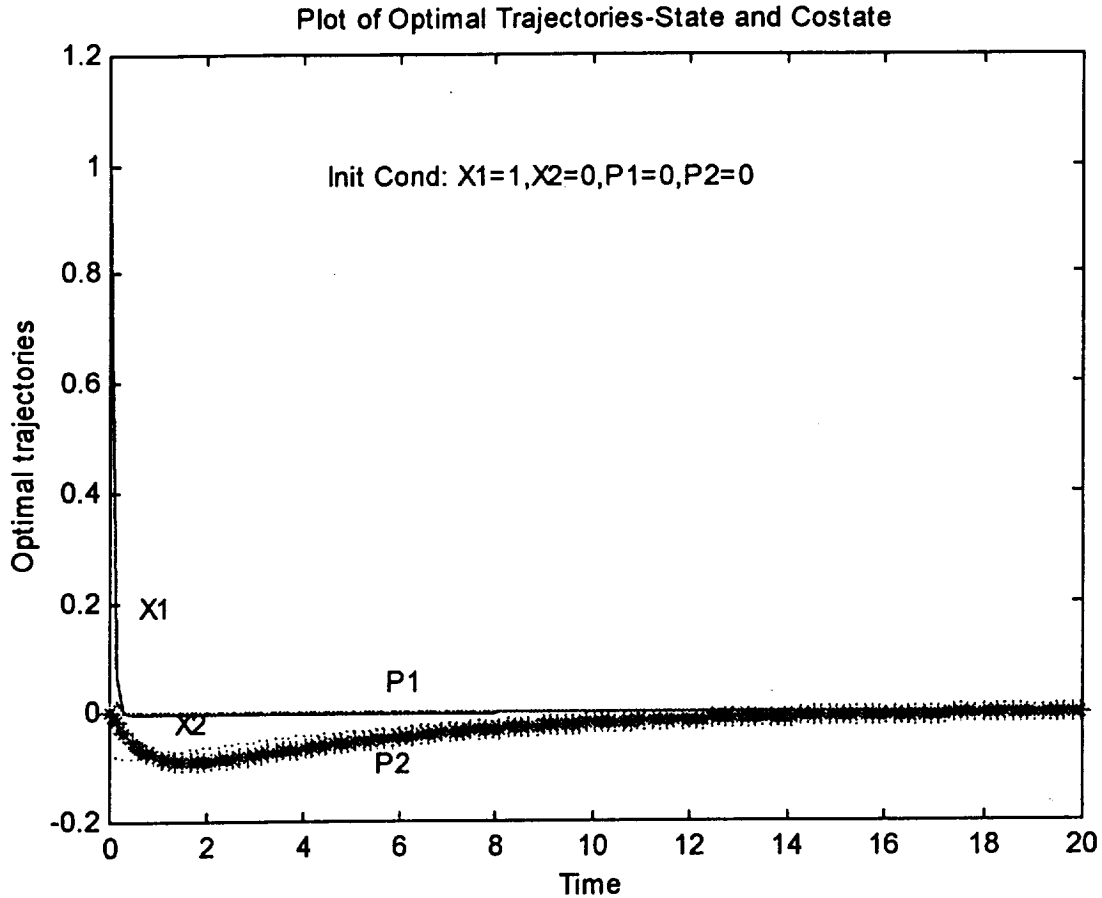
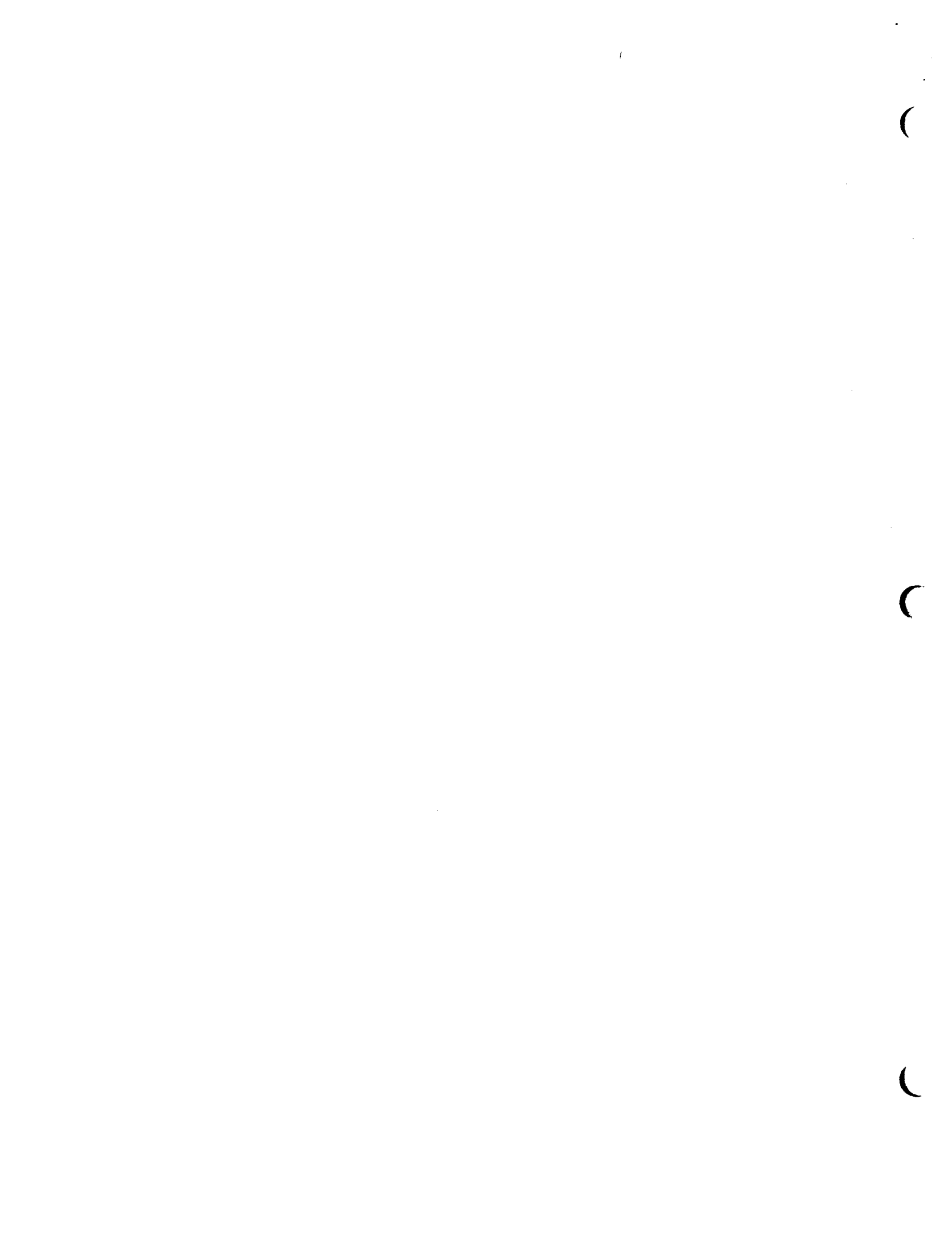


Figure (13) : Optimal Trajectories of State and Co-state vectors with different initial conditions.

Optimal trajectories can be plotted for various initial conditions. Figure (12) and (13) shows the trajectories for two such initial conditions. We can observe, by initializing x_1 and others equal to zero, that the optimal state and co-state trajectories reach steady state value quite quickly (around 14 seconds). This provides a very good tool to determine the behavior and to validate that the model is accurate enough.



4 - SIMULATION RESULTS

The results of a simulation of the nominal system in which no errors were detected is shown in Fig (14), and the dynamic threshold nicely brackets the MSE computation during the transient response periods. Figure (15) presents the same simulation data, showing the behavior of the threshold and MSE during the transient response between – and – seconds. Figure (16) is included to show what happens if the dynamic threshold value is not filtered to match the MSE, for this same nominal system. This figure demonstrates that the time lag due to filtering the MSE can cause a false detect if it is not compensated for in computation of the dynamic threshold [Ref: 11 and 13].

Various cases were studied with varying values of damping factor and the natural frequency of the model and the cases are discussed in the next section.

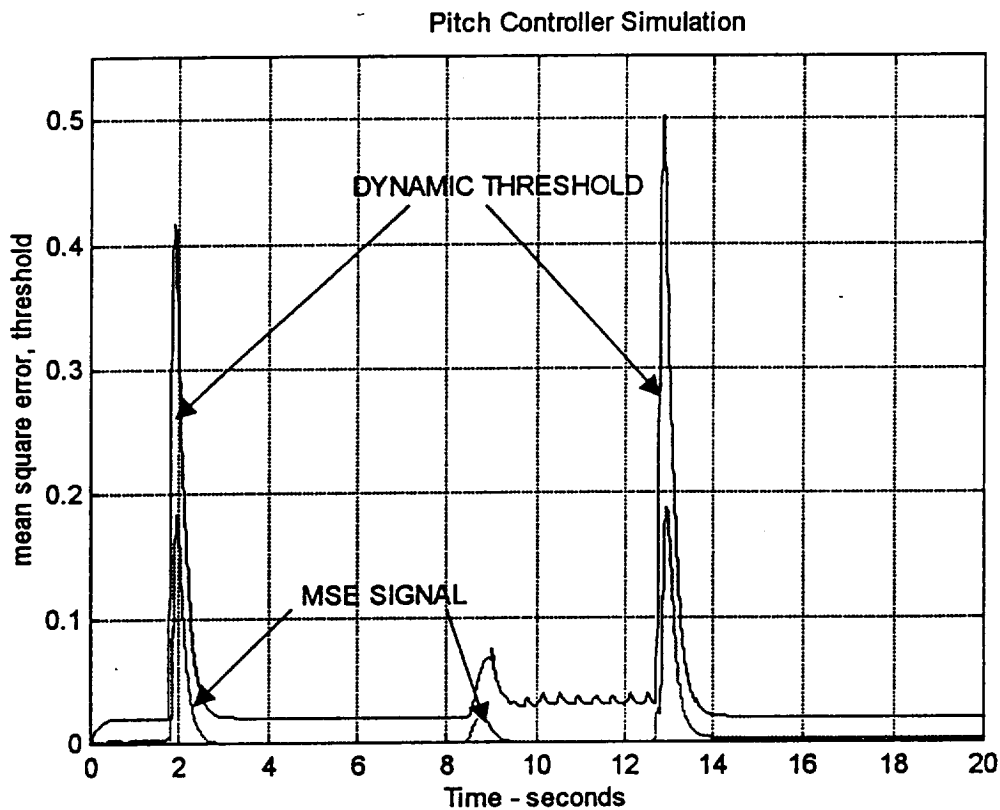


Figure (14): Pitch actuator controller simulation – nominal system – no abnormality.

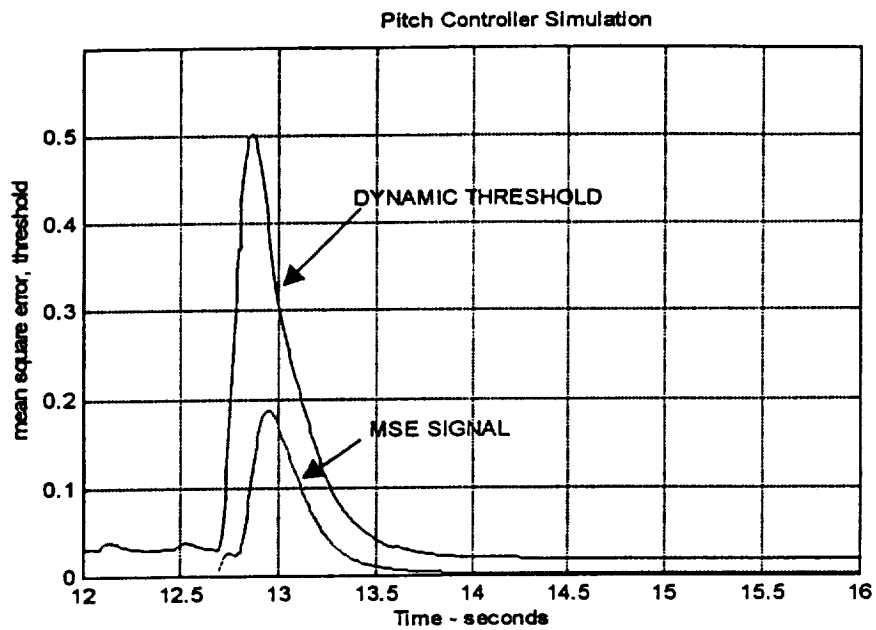


Figure (15): Pitch actuator controller simulation – filtered variable threshold – nominal system – no abnormalities – expanded view – ($\tau_1 = 0.02$, $\tau_2 = 0.04$)

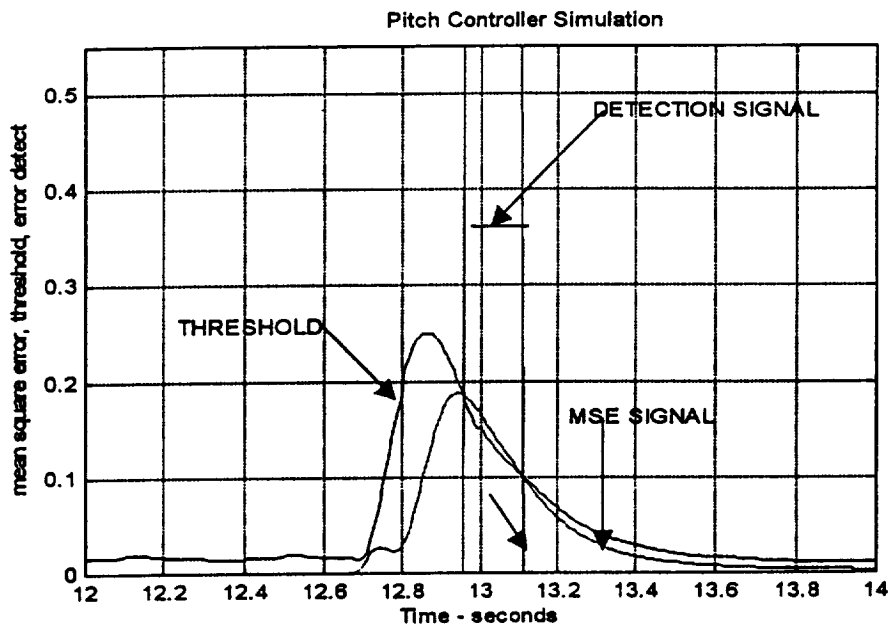


Figure (16): Pitch controller simulation – No filtering of variable threshold – ($\tau_1=0.05$, $\tau_2=0.02$)

It is noted here that the variations were made in the control parameters ζ , ω_n and k_s , to test this new innovation threshold idea. These control parameters have been shown to relate directly to the physical parameter of the System Under Test, therefore the detection of an abnormal control parameter will indicate an abnormal value of the physical parameter of the system under test.

Various figures were discussed to demonstrate the simulation of transient error in the system. In one of the demonstrations, different cases have been studied by varying the damping factor of the model. Figures show the actuator response, model response and error detection flag in each case. During all transient response periods, the error detection filter was able to successfully detect and announce the error. Various figures are also included to show the dynamic threshold, MSE and the error detect flag in detail for all the cases during the transient response periods.

In this case, variations were made in the damping ratio of the system by considering the characteristic equation of the transfer function. Figure (17) shows a case of 75% of the nominal damping ratio. Significance notice can be seen, such as increase in the overshoot of the model response, which corresponds to an error and we can see that the fault

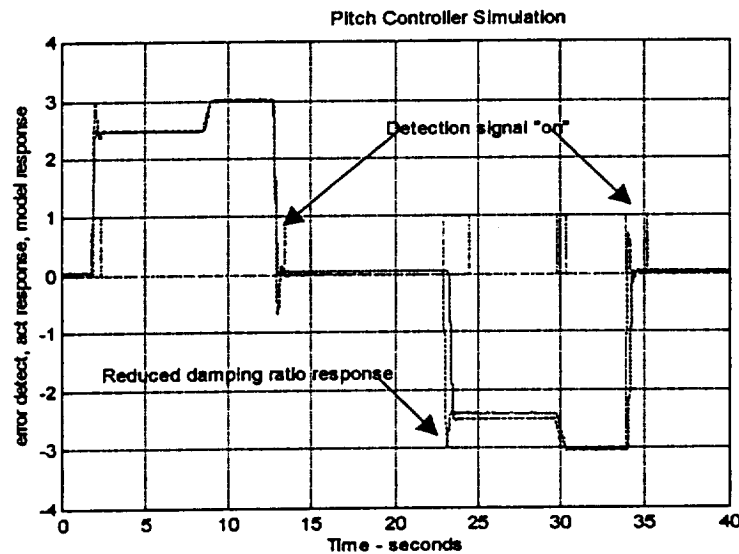


Figure (17): Pitch actuator controller simulation transient error is set at 75% of nominal damping ratio – Detection system signals abnormal response.

detection is “on”. Figure (18) shows an expanded view of this which clearly shows that there is a substantial increase in overshoot; hence the error filtered is triggered to give a detection signal.

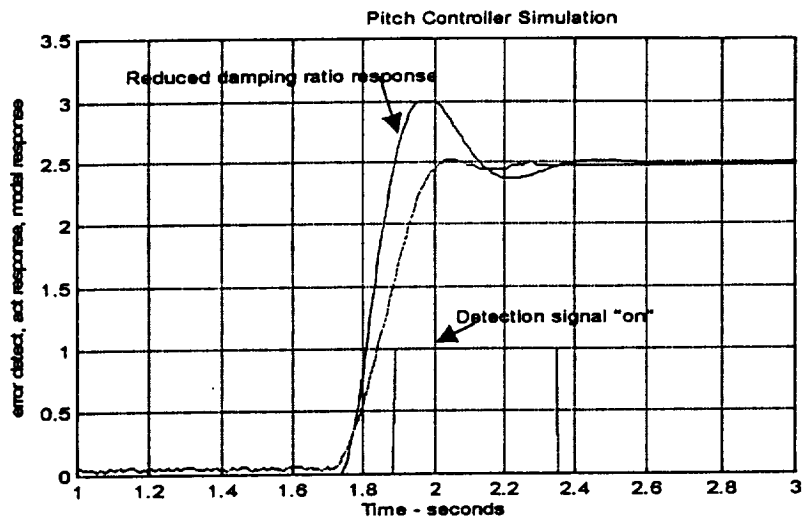


Figure (18): Pitch actuator controller simulation – Expanded view of 75% ζ_n .

Also Figure (19) shows Dynamic threshold vs Mean square error signal (MSE) where detection signal is on at the crossing of these two signals.

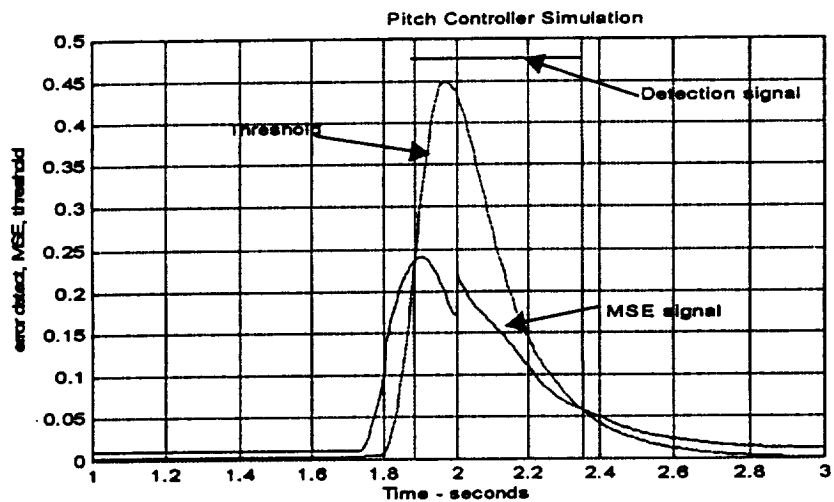


Figure (19): Pitch actuator controller simulation – Dynamic threshold vs error signal of 75% ζ_n .

Similar results can be noticed when the natural frequency of the system is varied. In all these cases, the error detection filter was able to detect and announce the error

successfully. We can also notice the changes in the model behavior; the transient response of the model is oscillatory and settling time is substantially increased (in the cases where the natural frequency is less than the nominal natural frequency). In the case of $\omega > \omega_n$, the error was detected to announce the change in the system parameters.

Overall, the error detection filter algorithm was able to determine the errors when the nominal parameters of the system was changed in both the directions (increasing and decreasing).

The basic idea behind all these different cases is the validation of the model and the success of the error detection filter to detect and announce error due to the changes in the system parameters. By this validation, we come to the conclusion that, if there is any abnormal measurement input/output data coming from the actual system under test, the model system parameters will change accordingly and due to these changes, the error detection filter will detect the faults, hence the basic goal of fault detection is achieved.



5. LIST OF REFERENCES

1. B. Friedland, *Control System Design*, McGraw Hill Publications, 1986.
2. Charles L. Phillips and Royce D. Harbor, *Feedback Control Systems*, Third Edition, Prentice Hall, 1996.
3. Roger W. Johnson, *A New Methodology for Launch/Spacecraft Vehicle Ground Health Management, Monitoring and Test and Evaluation (White Paper)*, Institute for Simulation and Training, University of Central Florida, April 29, 1994.
4. Roger W. Johnson, Sanjay Jayaram, Richard A Hull, *A New Real-Time Detection/Diagnosis Methodology for Automated Manufacturing*, University of Central Florida, 1998.
5. Arthur Gelb, Editor, *Applied Optimal Estimation*, The M.I.T Press, 1974.
6. Robert Grover Brown, Patrick Y.C. Hwang, *Introduction to Random Signals and Applied Kalman Filtering*, Third Edition, John Wiley and Sons, Inc., 1997.
7. Ron Patton, Paul Frank, Robert Clark, *Fault Diagnosis in Dynamic Systems – Theory and Application*, Prentice Hall International Inc., First Edition, 1989.
8. Donald E. Kirk, *Optimal Control Theory – An Introduction*, Prentice Hall International Inc., First Edition, 1970.
9. Richard C. Dorf, Robert H. Bishop, *Modern Control Systems*, Addison Wesley Longman Inc., Eighth Edition, 1998.
10. Bernard Friedland, *Maximum Likelihood Failure Detection of Aircraft Flight Control Sensors*, Journal of Guidance, Control and Dynamics, Vol. 5, No. 5, 1982, pp. 498-503.

11. John N. Little and Alan J. Laub, *Control System Toolbox for Use with MATLAB*, The Math Works Inc., Prentice Hall, 1996.
12. Lennart Ljung, *System Identification Toolbox for Use with MATLAB*, The Math Works Inc., Prentice Hall, 1997.
13. The Math Works Inc., *SIMULINK - Dynamic System Simulation Software*, User's Guide, 1993 and 1997.
14. The Math Works Inc., *MATLAB – High Performance Numeric Computation and Visualization Software*, 1993.

APPENDIX - A



98 OCT 15 AM 10 31